# The Inner Membrane Barrier of Lipid Membranes Experienced by the Valinomycin/$Rb^+$ Complex: Charge Pulse Experiments at High Membrane Voltages

Hermann Bihler and Günther Stark*
Department of Biology, University of Konstanz, Konstanz, Germany

ABSTRACT The kinetic analysis of charge pulse experiments at planar lipid membranes in the presence of macrocyclic ion carriers has been limited so far to the low voltage range, where, under certain simplifying conditions, an analytical solution is available. In the present study, initial voltages of up to 300 mV were applied to the membrane, and the voltage decay through the conductive pathways of the membrane was followed as a function of time. The system of differential equations derived from the transport model was solved numerically and was compared with the experimental data. The generalized kinetic analysis of charge pulse experiments and of steady-state current-voltage curves was used to study the voltage dependence of the individual transport steps and to obtain information on the shape of the inner membrane barrier. The data were found to be consistent with a comparatively broad inner barrier such as a trapezoidal barrier or an image force barrier. The inner barrier was found to sense 70–76% of the voltage applied to the membrane. As a consequence, 24–30% of the voltage acts on the two interfacial barriers between membrane and water. The data refer to membranes formed from monoolein, monoeicosenoin, or monoerucin in *n*-decane.

## INTRODUCTION

Lipid membranes are known to represent high dielectric barriers for the movement of simple inorganic ions such as $K^+$, $Na^+$, or $Cl^-$. As a consequence, their membrane permeability—in the absence of special transport systems—is extremely small. Certain organic ions, on the other hand, in which the charge is delocalized or shielded by hydrophobic groups, are able to cross the membrane at considerable rates. Typical examples are the lipophilic anions tetraphenylborate and dipicrylamine, or the positively charged monovalent complexes formed between $K^+$ and the ion carriers valinomycin and nonactin. The kinetics of their movement across lipid membranes has been studied in considerable detail in the past (for a review see Hladky, 1979, 1992; Läuger et al., 1981; Stark, 1984; Benz et al., 1989; Smejtek, 1995). The corresponding experiments are usually interpreted on the basis of a specific profile of the potential energy, which is characterized by minima near the two membrane/water interfaces and by a maximum in the center of the membrane. The profile (see Fig. 1) is the sum of different energetic contributions (Ketterer et al., 1971; Läuger et al., 1981): the image force experienced by any ion near the boundary of two different dielectric media, the hydrophobic interaction of the lipophilic ion with the membrane, the electrostatic interaction due to the interfacial potential at the membrane-solution interface, and energy terms arising from the distortion of the membrane structure around the ion.

Although there seems to be general agreement about the fundamental characteristics of the energy profile, the details of its shape are still unknown. The shape of the central barrier has been modeled by application of different approximations: 1) the Eyring barrier, a narrow and steep barrier in the middle of the membrane (Läuger and Stark, 1970); 2) the image force barrier, which is based solely on the calculation of the electrostatic energy of an ion near the membrane/water interface (Neumcke and Läuger, 1969; Haydon and Hladky, 1972; Andersen and Fuchs, 1975); and 3) the trapezoidal barrier (Hall et al., 1973; Hladky, 1974), which includes the rectangular barrier, which is valid for membranes of macroscopic dimensions. The different types of barriers have mainly been studied by considering their consequences for the description of the shape of current-voltage curves. Clear discrepancies between theory (based on the Eyring barrier) and experiments were observed at large membrane voltages (Stark and Benz, 1971), whereas theories based on image force or trapezoidal barriers show better agreement with the experimental data (Hall et al., 1973; Hladky, 1974; Andersen and Fuchs, 1975; Krasne and Eisenman, 1976; Ciani, 1976; Benz and McLaughlin, 1983).

In the present communication, the charge pulse method, a fast kinetic technique, in combination with steady-state current-voltage curves, is applied to study the voltage dependence of the rate of ion translocation across the central barrier. This allows one to investigate the problem in question in a more extensive way. So far, charge pulse experiments have been analyzed within the limits of small membrane voltages only, where analytical solutions of the problem are available (Benz and Läuger, 1976; Benz et al., 1976). At high membrane voltages, the analysis has hitherto

*Received for publication 2 December 1996 and in final form 17 April 1997.*
Address reprint requests to Dr. G. Stark, Fakultät für Biologie, Universität Konstanz, Postfach 55 60 M638, D-78434 Konstanz, Germany. Tel.: 49-75-31-88-22-89; Fax: 49-75-31--88-31-83; E-mail: gunther.stark@uni-konstanz.de.

0006-3495/97/08/746/11 $2.00

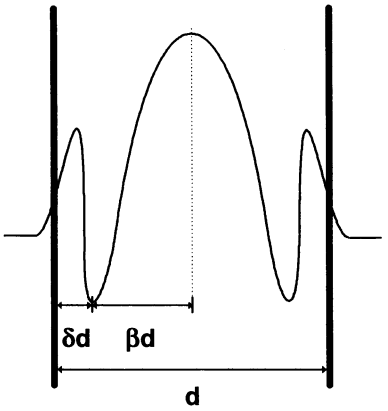


FIGURE 1 Schematic representation of the potential energy experienced by lipophilic organic ions or by hydrophobic ion carrier complexes during their passage through a membrane of thickness $d$.

been restricted to the steady-state domain (Feldberg and Kissel, 1975), which does not allow determination of individual rate constants. In the present study the relevant set of differential equations (under the conditions of a charge pulse experiment) is numerically integrated, and the result is compared with the time-dependent decay of the membrane voltage. The latter is found to depend on the shape of the membrane barrier (if sufficiently high membrane voltages are applied). Thus the first complete solution of the charge pulse problem independent of the value of the membrane voltage is obtained. The generalized kinetic analysis is applied to study rubidium transport mediated by the macrocyclic ion carrier valinomycin across lipid membranes formed from monoglycerides. The voltage dependence of the individual transport steps and the shape of the inner membrane barrier are the main issues investigated.

## MATERIALS AND METHODS

### Membrane formation

Planar lipid membranes of the Mueller-Rudin type were formed from three different monoglycerides (Nu Chek Prep, Elysian, MN) dissolved in *n*-decane (standard for gas chromatography; Fluka, Buchs, Switzerland): monoolein (18:1 MG), monoeicosenoin (20:1 MG), and monoerucin (22:1 MG). In addition, the membrane-forming solution contained $5 \times 10^{-4}$ M valinomycin (Boehringer Mannheim, Mannheim, Germany). Most of the experiments were performed with 1 M RbCl (pH 5.6, unbuffered) in the aqueous solutions surrounding the membrane. The temperature was 20°C throughout.

### Current-voltage relationship

Current-voltage curves were measured by the application of a voltage ramp from a function generator (model 90; Wavetek, San Diego, CA). Both the current and the voltage signal, after appropriate amplification, were fed into an IBM-compatible computer equipped with an analog/digital board DAS-1600 (Keithly MetraByte, Taunton, MA). A series of precautions were taken into account to ensure that the measurements reflected the steady-state current-voltage behavior (see Bihler, 1996, for details): 1) The frequency of the ramp ($f$ = 1 Hz) was many orders of magnitude smaller than the frequency range of the (non-steady-state) specific relaxations of the carrier system investigated (see below). 2) The capacitive current $I_c = C_m\, dV_m/dt + V_m\, dC_m/dt$ ($C_m$ = membrane capacity, $V_m$ = membrane voltage) was found to be negligible under the conditions applied, i.e., $I = I_i + I_c \approx I_i$ ($I_i$ = ionic current). 3) The conversion-delay of the analog/digital converter between subsequent current and voltage data was corrected for. Measurements were performed using membranes of 1-mm diameter. The signal-to-noise ratio was improved by the averaging of 100 signals.

### Charge-pulse experiments

Charge pulses were supplied to the membrane by a new technique that was described recently (Barth et al., 1995; Hladky et al., 1995; Bihler, 1996). The method is based on the capacitive coupling of a voltage jump of amplitude, $V$, at time $t = 0$ to the membrane (cf. Fig. 2). As a consequence (because $C_c \ll C_m$), a charge pulse $\Delta Q = VC_c$ is transferred to the membrane capacity, $C_m$, at $t = 0$. The resulting membrane voltage, $V_m^0 = VC_c/C_m$, in view of the conductive pathways of the membrane, will subsequently decay to zero. If the membrane is approximated by a parallel arrangement of capacity, $C_m$, and resistance, $R_m$, the time dependence of $V_m$ is given by the simple relation

$$V_m(t) = V(C_c/C_m)\exp(-t/R_mC_m) \qquad (1)$$

Measurement of the initial voltage, $V_m^0 = VC_c/C_m$, allows determination of the membrane capacity, $C_m$. If the membrane is doped with a special transport system, the time dependence, $V_m(t)$, contains information about the specific relaxation processes of the system. The shape of the function, $V_m(t)$, may be used to derive the parameters of the transport model in this case (see below).

The time resolution of the method is determined by the time interval necessary for the transfer of the initial charge, $\Delta Q$, to the membrane and by the bandwidth of the applied instrumentation. The time interval is limited by the series resistance, $R_s$, to the membrane. The characteristic time constant $R_sC_c$ of the charge transfer may be reduced to the order of a nanosecond with our present instrumentation (Barth et al., 1995; Bihler, 1996). The value holds for comparatively small membrane voltages. At the high voltages applied throughout the present study, the time resolution is impaired by about an order of magnitude. This is caused by the larger value of the coupling capacity, $C_c$, required. For initial membrane voltages on the order of 200–300 mV, the charge transfer was found to be completed after ~200–300 ns.

The method implies that the decay of $V_m$ is due to the conductive pathways of the membrane only (i.e., charge transfer through the external electronic circuit must be negligible). Therefore, the preamplifier, apart from a sufficient bandwidth, must have a sufficiently high impedance. The preamplifier used throughout the present study was built in the electronic

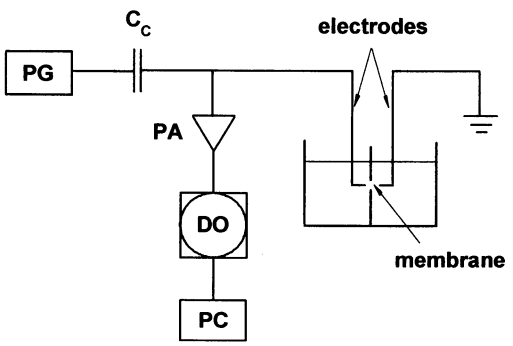


FIGURE 2 Charge-pulse technique based on capacitive coupling (capacity $C_C$) of a voltage jump from a pulse generator (PG) to a lipid membrane (Barth et al., 1995). The time-dependent voltage difference between the two electrodes is detected by a high-impedance preamplifier (PA), stored in a digital oscilloscope (DO), and finally transferred to the computer (PC).

workshop of our university (bandwidth 20 MHz, input resistance $10^{11}$ Ω, gain 10-fold). The digital oscilloscope applied (Tektronix 7903/7D20) had a memory size of 1024 words. Because $V_m(t)$ extends over several orders of magnitude in time (cf. Fig. 4), the different time ranges of the signal had to be measured successively. The complete signal was subsequently assembled in the computer. Data analysis was performed using the software package Asyst (Keithly MetraByte).

## THE CARRIER MODEL AND ITS ANALYSIS

### Carrier model

The transport of monovalent cations, $M^+$, by neutral, macrocyclic ion carriers, S, of the valinomycin type is due to 1:1 complexes, $MS^+$, formed near the membrane/water interface. Numerous experiments were found to be largely consistent with a simple reaction scheme shown in Fig. 3 (for a review see Hladky, 1979, 1992; Läuger et al., 1981; Stark, 1984; Benz et al., 1989). It is based on profiles of the potential energy depicted in Fig. 1. Similar profiles (although of different barrier heights or widths) are assumed to hold for both carrier species S and $MS^+$. In view of the steep energy barriers, species $MS^+$ and S are largely confined to the two minima at a distance, $\delta d$, from the aqueous phase. If the concentrations of S and $MS^+$ outside the minima are neglected, the scheme may be treated according to the formalism of chemical kinetics, i.e., the relative interfacial concentrations $n'_S$, $n''_S$, $n'_{MS}$, and $n''_{MS}$ ($n_i^k = N_i^k/N_0$, $N_i^k$ = interfacial concentrations, $N_0$ = total carrier concentration) are related to each other by rate equations. Both complex formation and dissociation as well as translocation of species S and $MS^+$ across the inner membrane barrier are described by appropriate rate constants:

$$n'_S + n''_S + n'_{MS} + n''_{MS} = 1 \tag{2}$$

$$\frac{dn'_S}{dt} = -(k_R c'_M + 2k_S)\cdot n'_S + (k_D - k_S)\cdot n'_{MS} - k_S n''_{MS} + k_S \tag{3}$$

$$\frac{dn'_{MS}}{dt} = k_R c'_M \cdot n'_S - (k_D + k'_{MS})\cdot n'_{MS} + k''_{MS}\cdot n''_{MS} \tag{4}$$

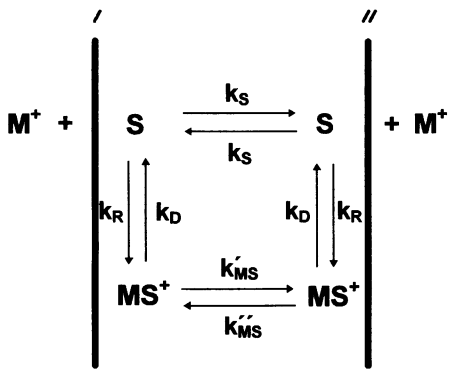


FIGURE 3 Reaction scheme of the transport of cations $M^+$ mediated by macrocyclic carrier molecules S of the valinomycin type (Läuger and Stark, 1970).

$$\frac{dn''_{MS}}{dt} = -k_R c''_M \cdot n'_S + (k'_{MS} - k_R c''_M)\cdot n'_{MS} - (k''_{MS} + k_D + k_R c''_M)\cdot n''_{MS} + k_R c''_M \tag{5}$$

$c'_M$ and $c''_M$ represent the ion concentrations at the place of complex formation (i.e., at the minima of the energy profile; see below).

The voltage dependence of the transport model is introduced as follows (see Knoll and Stark, 1975, and the Discussion for justification). The membrane voltage, $V_m$, changes the shape of the inner membrane barrier. As a consequence, the rate constants of translocation in opposite directions, $k'_{MS}$ and $k''_{MS}$, of the positively charged complexes, $MS^+$, are increased and decreased, respectively. Modified Eyring relations were applied to account for the voltage dependence, i.e.,

$$k'_{MS} = k_{MS}\cdot e^{\beta u}\cdot f(u) \tag{6}$$

$$k''_{MS} = k_{MS}\cdot e^{-\beta u}\cdot f(u) \tag{7}$$

with

$$f(u) = \frac{1+g}{g+(1+u)^h} \tag{8}$$

$u = FV_m/RT$ is the reduced voltage ($F$, Faraday constant; $R$, gas constant). $g$, $h$, and $\beta$ are free parameters to be determined experimentally. For $h = 0$ (i.e., $f(u) = 1$), Eqs. 6–8 describe ion translocation across the Eyring barrier, a steep and narrow barrier in the middle of the membrane (Läuger and Stark, 1970). For $h > 0$ (i.e., $f(u) < 1$ for $u > 0$), Eq. 8 represents a correction function to account for broader barrier shapes, as compared with the Eyring barrier (see Discussion).

For $\beta = 0.5$, translocation of $MS^+$ is the only voltage-dependent process. For $\beta < 0$ (i.e., $\delta > 0$; cf. Fig. 1), the interfacial reaction becomes voltage dependent. This may be accounted for in different ways, either by the introduction of voltage-dependent rate constants of complex formation and dissociation (Hladky, 1974), or by the assumption of voltage-dependent ion concentrations, $c'_M$ and $c''_M$, at the place of complex formation (i.e., at the minima of the potential energy; cf. Knoll and Stark, 1975). The latter alternative has been selected in the present study. By introduction of a voltage-dependent partition coefficient, $\gamma_M$, the concentrations $c'_M$ and $c''_M$ are obtained as

$$c'_M = \gamma'_M c_M = \gamma^0_M e^{\delta u} c_M \tag{9}$$

$$c''_M = \gamma''_M c_M = \gamma^0_M e^{-\delta u} c_M \tag{10}$$

$$\delta = 0.5 - \beta \tag{11}$$

$\gamma^0_M$ is the partition coefficient for $u = 0$. The rate constants $k_R$, $k_D$, and $k_S$ are assumed to be voltage independent.

The current, $I$, detected in the external circuit at a constant membrane voltage, $V_m$, is determined by the transition rates, $\Phi_\nu$, of ion translocation across the different barriers of the energy profile according to (Läuger et al., 1981)

$$I = e_0 \sum_\nu \alpha_\nu \Phi_\nu \tag{12}$$

If a constant dielectric constant, $\epsilon$, is assumed inside the membrane, the displacement coefficients, $\alpha_\nu$, are given by

$$\alpha_\nu = z \frac{a_\nu}{d} \tag{13}$$

where $z$ is valency, and $a_\nu$ are the distances between the different energy minima.

In the case of charge pulse experiments (i.e., at zero current in the external circuit), the relation

$$\frac{dV_m}{dt} = -\frac{e_0}{C_m} \sum_\nu \alpha_\nu \Phi_\nu \tag{14}$$

holds ($C_m$ is the membrane capacity). Läuger et al. (1981) should be consulted for the derivation of Eqs. 12–14. Application of Eqs. 13–14 to the reaction scheme (cf. Fig. 3) yields the following result for the time derivative of the reduced voltage, $u$ (instead of $V_m$):

$$\frac{du}{dt} = -\frac{F^2 N_0}{RTC_m} \left\{ \begin{array}{l} \delta \cdot (k_R c_M \gamma'_M \cdot n'_S - k_D \cdot n'_{MS}) \\ + 2\beta \cdot (k'_{MS} \cdot n'_{MS} - k''_{MS} \cdot n''_{MS}) + \\ \qquad \delta \cdot (k_D \cdot n''_{MS} - k_R c_M \gamma''_M \cdot n''_S) \end{array} \right\} \tag{15}$$

Charge-pulse experiments were analyzed using the initial conditions

$$n'_{MS} = n''_{MS} = n_{MS} \tag{16}$$

$$n'_S = n''_S = n_S \tag{17}$$

and

$$\frac{n_{MS}}{n_S} = \frac{k^0_R c_M}{k_D} \qquad k^0_R = k_R \gamma^0_M \tag{18}$$

## Analysis

### *Current-voltage relationship*

Instead of the current, $I$, the steady-state conductance, $\lambda = I/V_m$, is analyzed as a function of the reduced voltage, $u$. By applying Eq. 12 in combination with Eqs. 2–11 and 13, the following result is obtained ($\lambda_0 = \lambda(u \to 0)$):

$$\frac{\lambda(u)}{\lambda_0} = \frac{2 \cdot f(u) \cdot \sinh(u/2) \cdot A_1}{u \cdot [A_2 + A_3 + A_4 + A_5]} \tag{19}$$

with

$$A_1 = (1 + 2z + yzc_M) \cdot (1 + xc_M)$$

$$A_2 = xzc_M f(u) \cosh(\beta u) \cdot (2 \cosh(\delta u) + yc_M)$$

$$A_3 = yzc_M f(u) \cosh(u/2)$$

$$A_4 = 2zf(u) \cosh(\beta u)$$

$$A_5 = 1 + xc_M \cosh(\delta u)$$

and

$$x = \frac{k^0_R}{k_D}, \quad y = \frac{k^0_R}{k_S}, \quad z = \frac{k_{MS}}{k_D}$$

$f(u)$ is defined via Eq. 8.

Equation 19 contains information about the correction function $f(u)$ and on the width, $2\beta$, of the inner barrier. Depending on the size of the parameters $x$, $y$, and $z$, the reduced conductance, $\lambda(u)/\lambda_0$, either increases or decreases with $u$. In certain limiting cases, Eq. 19 is completely determined either by $f(u)$ or by $\beta$. This is shown by considering sufficiently small concentrations, $c_M$. By using this assumption, Eq. 19 is reduced to

$$\frac{\lambda(u)}{\lambda_0} = \frac{2(1 + 2z) f(u) \sinh(u/2)}{u[1 + 2zf(u) \cosh(\beta u)]} \tag{20}$$

1. If $2z \ll 1$, $\lambda(u)/\lambda_0 = 2f(u)\sinh(u/2)/u$ depends on the correction function $f(u)$ only. As a consequence, $f(u)$ may be derived from experimentally determined current-voltage curves under these conditions.

2. By assuming $2z \gg 1$, Eq. 20 is reduced to $\lambda(u)/\lambda_0 = 2 \sinh(u/2)/(u \cos(\beta u))$. The relative distances $\beta$ (and $\delta$; cf. Eq. 11) may be easily determined in this case.

The same result is obtained at arbitrary concentrations, $c_M$, but at sufficiently small values of $x$ and $y$.

### *Charge-pulse experiments*

The analysis consists in the solution of the system of differential equations (Eqs. 3–5 and 15, including Eqs. 2 and 6–11), and the initial conditions (Eqs. 16–18). Benz and Läuger (1976) have shown that the problem has an analytical solution, if ion translocation by the carrier is the only voltage-dependent process (i.e., $\beta = 0.5$), and if the analysis is restricted to the low voltage range (so that $f(u) = 1$ and $\exp(\pm u)$ can be replaced by $(1 \pm u)$). In that case, $V_m(t)$ is obtained as a sum of three exponential terms, i.e.,

$$V_m(t) = V^0_m(a_1 \exp(-t/\tau_1) + a_2 \exp(-t/\tau_2) + a_3 \exp(-t/\tau_3)) \tag{21}$$

$$a_1 + a_2 + a_3 = 1$$

The three relaxation times, $\tau_1$, $\tau_2$, and $\tau_3$, and the two independent relaxation amplitudes, $a_1$ and $a_2$, depend on the four rate constants $k_R$, $k_D$, $k_{MS}$, and $k_S$ of the carrier model

and on the total concentration, $N_0$, inside the membrane. The reader should consult Benz and Läuger (1976) for the detailed equations and for the procedure, which allows determination of the model parameters under these conditions. The practical aspects of data analysis have been described in a recent publication (Barth et al., 1995).

If $\beta < 0.5$ (or $u \geq 1$), the problem must be solved numerically. This was done as follows. The variables $V_i$ (i.e., $n'_S$, $n''_S$, $n'_{MS}$, $n''_{MS}$, and $u$) were obtained by a Runge-Kutta procedure. The values of the five model parameters $P_i$ (i.e., of $k_R$, $k_D$, $k_S$, $k_{MS}$, and $N_0$) were selected from the analytical solution obtained for $\beta = 0.5$ and $u < 1$. The goodness of the fit ($\chi^2$) was tested by calculation of the sum of the squares of deviations from the data. $\chi^2$ was minimized by a random procedure of data simulation. Random numbers $Z_i$ were generated in the interval $-1$ to $+1$, and the model parameters $P_i$ were replaced by $P_i(1 + Z_i * S)$. $S$ represents a free selectable step size ($0 < S < 1$) common to all parameters $P_i$. In the case of an improvement of $\chi^2$, the new parameters were selected as starting values and the procedure was repeated. If $\chi^2$ did not improve, the old parameters were used as starting values and new random numbers were generated. After a certain number of unsuccessful trials of improvement, the step size was reduced (because the minimum of $\chi^2$ was assumed to be in the close neighborhood of the set of parameters chosen). Typically some $10^3$ simulations had to be performed to obtain satisfactory agreement between theory and experimental data. About 150 digital data were used for the fitting procedure. The data were selected at equidistant time intervals. Because the decay of $V_m$ extends over three to four orders of magnitude in time, the size of the intervals was changed three times to adjust to the different time domains of the decay. Calculations were performed with the software package Asyst. To increase the speed of simulation, a FORTRAN routine of the Runge-Kutta procedure was interfaced to Asyst. For further details see Bihler (1996).

### *Determination of the correction function f(u)*

The charge-pulse relaxation data could be fitted by a broad range of different $\beta$-values. Therefore, $\beta$ was determined via the shape of the current-voltage relationship (see above). Further analysis was as follows. Charge-pulse experiments were performed at small membrane voltages (i.e., $u < 1$) and at high membrane voltages (i.e., $u = 6$–$12$) at the same membrane. By using the low voltage data, the model parameters were determined as described under point 2). Simulation of the high voltage data was performed by using the model parameters obtained from the low voltage data. For $f(u) = 1$, a clear discrepancy between data and simulation was observed (cf. Fig. 4). Therefore, Eq. 8 was applied. By using a simple algorithm, the parameters $g$ and $h$ of $f(u)$ were adjusted in such a way as to obtain an optimum fit to the data.

## RESULTS

Charge-pulse experiments at lipid membranes formed from monoglycerides in the presence of valinomycin have been found to agree with Eq. 21, provided the initial voltage was small enough and the voltage dependence of the interfacial reaction was neglected (Benz and Läuger, 1976; Barth et al., 1995; Hladky et al., 1995). Detection of the three relaxation times and the corresponding amplitudes allows one to determine the four rate constants of the model and the total carrier concentration inside the membrane. The good agreement between theory and experiment is limited, however, to the low voltage range. Independent of the detailed shape of the inner barrier, $k'_{MS}$ and $k''_{MS}$ are linearly dependent on the voltage, $u$, in this case. The deviations between theory and experiment observed at high initial membrane voltage are illustrated in Fig. 4. A charge pulse of sufficient amplitude was applied to obtain an initial voltage, $V^0_m$, of 200 mV. The decay of $V^0_m$ extends over more than four orders of magnitude to virtually zero. The dashed line was calculated on the basis of low voltage data from the same membrane, assuming $f(u) = 1$. Clear discrepancies are observed in the time domain up to 30 $\mu$s, and there was good agreement over the complete time range in the case of the low voltage experiment (data not shown). The deviations disappear if the translocation rate constants $k'_{MS}$ and $k''_{MS}$ are corrected for a barrier shape different from the Eyring barrier, i.e., if Eq. 8 is applied with appropriate values of the parameters $g$ and $h$ (determined via the fitting procedure described in the previous section). Fig. 4 also shows the time dependence of the relative interfacial concentrations $n'_S$, $n''_S$, $n'_{MS}$, and $n''_{MS}$. Starting with identical values at the two interfaces, the concentrations are increased at one interface ($''$) and diminished at the other ($'$). The asymmetry is induced by the stepwise generation of the initial membrane voltage, $V^0_m$, and is subsequently reduced to zero as the membrane capacity is discharged by carrier-mediated ion transport through the membrane. All of the curves were obtained by numerical integration of the relevant set of the differential equations (see last section).

The decay, $V_m(t)$, of the membrane voltage could be fitted with sufficient accuracy by using different values of $\beta$ ($\beta \leq 0.5$), i.e., $V_m(t)$ was found to be rather insensitive to the distance, $\beta d$, between the two energy minima (see Fig. 1). Therefore $\beta$ was obtained by analysis of the current-voltage relationship. The procedure was as follows. Charge-pulse experiments were fitted for different values of $\beta$. The rate constants obtained (together with the $\beta$-value selected) were used to compare Eq. 19 with current-voltage curves determined experimentally (cf. Fig. 5). In the case of membranes formed from 20:1 MG, there is fairly good agreement with the theory for $\beta \approx 0.38$. The small discrepances observed at voltages $V_m > 0.1$ V may be caused by the effects of electrostriction (leading to an enlargement of the membrane area and to a reduction of the membrane thickness). The reduced conductance, $\lambda(u)/\lambda_0$, is found to decrease with increasing voltage (equivalent to a saturating current-volt-

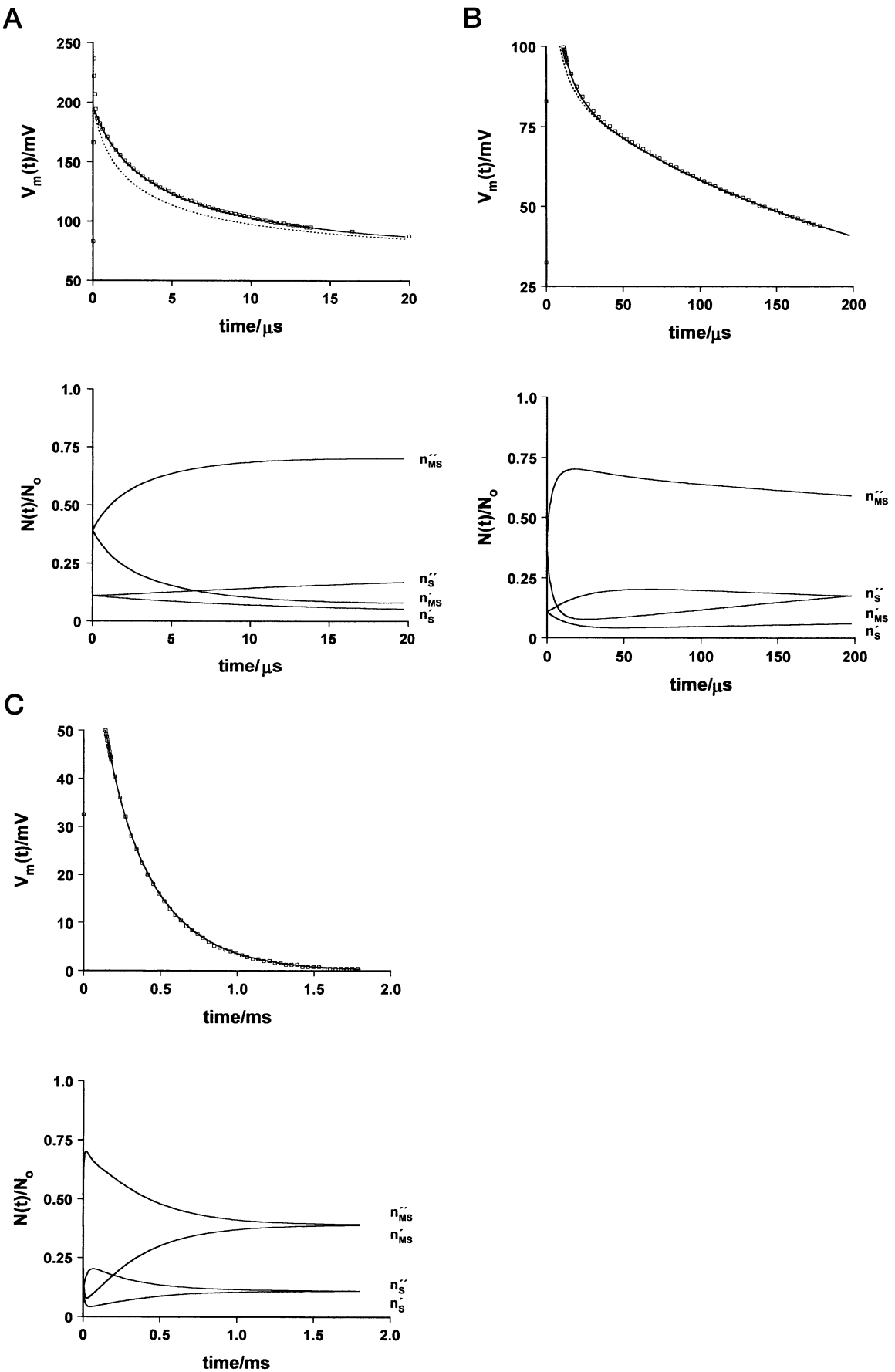
A
B
C
$V_m(t)$/mV
time/μs
time/ms
N(t)/N$_o$
$n''_{MS}$
$n''_S$
$n'_{MS}$
$n'_S$

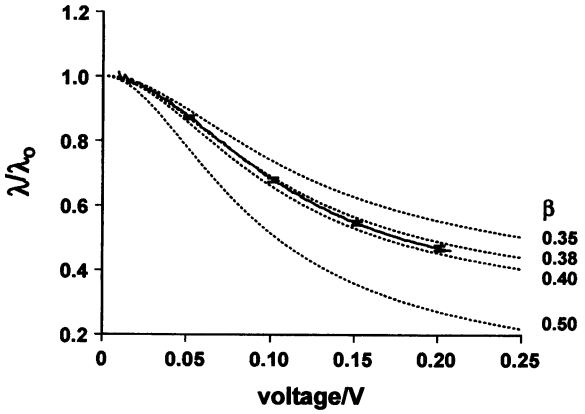


FIGURE 5 Current-voltage relationship of membranes formed from 20:1 MG in *n*-decane (containing $5 \times 10^{-4}$ M valinomycin) in the presence of 1 M RbCl in the aqueous phase. Instead of the current, the conductance $\lambda$, devided by the conductance $\lambda_0$ (obtained for $V_m \rightarrow 0$), is plotted as a function of voltage $V_m$. The solid line consists of $10^3$ digital data and represents mean values of five different membranes. The error bars at four selected data show the standard deviation. The dashed lines were calculated from Eq. 19. The values of the parameter, $\beta$, are indicated.

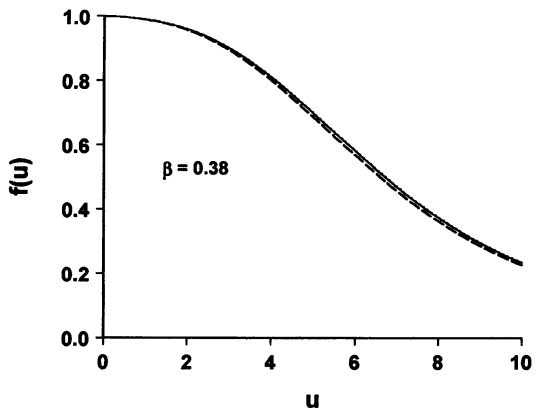


FIGURE 6 Shape of the correction function $f(u)$ for the valinomycin/$Rb^+$ complex. The three (nearly coincident) lines were obtained from charge pulse experiments (cf. Fig. 4) at three different initial voltages of 150 mV, 200 mV, and 250 mV. The measurements were performed at a single membrane formed from 22:1 MG. $f(u)$ was calculated according to Eq. 8. For mean values of the parameters $g$ and $h$, see Table 4.

age curve). The shape of the current-voltage relation is largely determined by the value of $\beta$ under these conditions, i.e., it is hardly affected by the correction function $f(u)$ (see discussion of Eq. 20).

The analysis allows the determination of all model parameters and was carried out for monoglyceride membranes of different chain lengths of their fatty acid residues (i.e., different membrane thickness). Figs. 6 and 7 illustrate the shape of the correction function $f(u)$. The shape is found to be independent of the initial voltage applied. The deviation from the behavior of an ideal Eyring barrier (i.e., $f(u) = 1$) increases with the applied voltage. The deviation is larger for 22:1 MG as compared with 20:1 MG. In the case of 18:1 MG, the charge pulse data could be fitte by different functions $f(u)$, i.e., the definite shape of $f(u)$ could not be determined.

Tables 1–4 summarize the values of the model parameters obtained. $\beta$ was definitely found to be smaller than 0.5. The value used for numerical analysis of the charge pulse experiments (i.e., 0.35 and 0.38; cf. Table 3) represent the best estimates obtained from current-voltage curves. The rate constants found for different $\beta$-values differ by less than a factor of 2 from the previous analysis (Benz and Läuger, 1976), which was based on the analytical solution, assuming $\beta = 0.5$ (compare Tables 2 and 3). The constants, $g$ and $h$, which determine the shape of $f(u)$, are summarized in Table 4. They represent a fit of Eq. 8 to the mean value of six independent determinations of $f(u)$. The $\beta$ values obtained indicate that 70–76% of the voltage applied to monoglyceride membranes (of chain length 18:1 to 22:1) drop across the inner barrier. As a consequence, 24–30% of the voltage acts on the two interfacial barriers between membrane and water.

Similar experiments were performed at smaller $Rb^+$ concentrations in water. The amplitudes of the specific relaxation processes of the carrier model (and, as a consequence, the accuracy of the resulting interpretation) are, however, considerably reduced under these conditions (data not shown).

## DISCUSSION

The movement of lipophilic molecules across the central barrier of lipid membranes has been described in different ways. In applying the classical approach of electrodiffusion, the ion flux, $\Phi$, over the barrier is given by a generalized Nernst-Planck equation (Neumcke and Läuger, 1969; Benz

FIGURE 4 Time dependence of the membrane voltage, $V_m$, and of the (relative) interfacial concentrations $n'_{MS}$, $n''_{MS}$, $n'_S$, and $n''_S$ in a charge pulse experiment. The membrane voltage, after completion of the initial voltage spike, was ~200 mV. The decay of $V_m$ (and the variation of the interfacial concentrations) is shown at three different time scales (Fig. 4 *A–C*). The experiment was performed by application of a voltage jump of amplitude 1.16 V to a membrane (of ~0.6 mm diameter) formed from 20:1 MG in *n*-decane (containing $5 \times 10^{-4}$M valinomycin) in the presence of 1 M RbCl in the aqueous phase (coupling capacity $C_C = 224$ pF, membrane capacity $C_m = 1.09$ nF). The lines correspond to numerical calculations using $V_m^0 = 197$ mV, and the following values: $k_{MS} = 3.25 \times 10^4\ s^{-1}$, $k_S = 0.82 \times 10^4\ s^{-1}$, $k_R = 3.65 \times 10^4\ M^{-1}\ s^{-1}$, $k_D = 1.02 \times 10^4\ s^{-1}$, $N_0 = 1.55 \times 10^{-12}$ mol $cm^{-2}$, and $\beta = 0.38$. These values (as well as the value of the membrane capacity, $C_m$) were obtained from a charge pulse experiment with the same membrane but at sufficiently low membrane voltage ($f(u) = 1$ in this case; see text for details; data not shown). The dashed line was calculated for $f(u) = 1$, but for the high membrane voltage, $V_m^0 = 197$ mV, applied at the experiment illustrated. The solid line was adjusted to the data by using a voltage-dependent $f(u)$ according to Eq. 8. The best fit was obtained for $g = 131$ and $h = 2.15$. The latter data were also applied to the calculation of the time dependence of the interfacial concentrations $n'_{MS}$, $n''_{MS}$, $n'_S$, and $n''_S$.

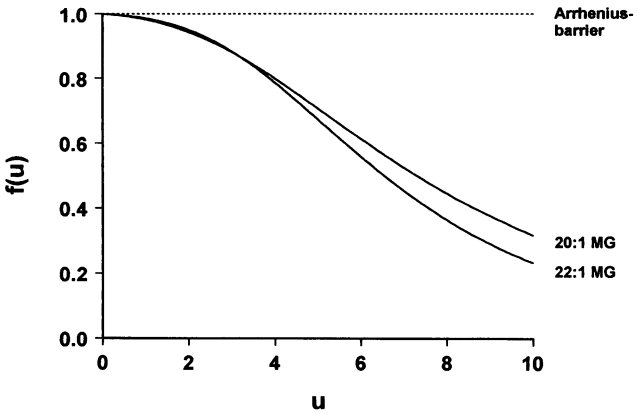


FIGURE 7 Comparison of the correction function $f(u)$ for an Arrhenius type of barrier (usually designated as an Eyring barrier; cf. Zwolinski et al., 1949) and for the barrier of the two kinds of monoolein membranes investigated.

et al., 1976):

$$\Phi = -D\left(\frac{dC}{dx} + zC\frac{d\varphi}{dx} + C\frac{dw}{dx}\right) \tag{22}$$

$D(x)$ is the diffusion coefficient and $C(x)$ is the concentration of the permeable ion in the membrane. $X$ represents the space coordinate perpendicular to the membrane, $\varphi(x) = F\phi(x)/RT$ is the reduced electrical potential ($\phi(x)$ = electrical potential), and $w(x)$ is the potential energy (expressed in units of $RT$) of the ion at $u = 0$. Under steady-state conditions, Eq. 22 may be integrated to give

$$\Phi = \frac{C(-\beta d)h(-\beta d) - C(\beta d)h(\beta d)}{\int_{-\beta d}^{\beta d}[h(x)/D(x)]dx} \tag{23}$$

with $h(x) = \exp(z\varphi(x) + w(x)$ (cf. also Fig. 1).

The Nernst-Planck approach has a series of limitations. The shape of the potential energy $w(x)$ and the function, $D(x)$, are unknown. The diffusion coefficient, $D$, is not a constant but will depend on the coordinate $x$, i.e., on the position inside the layer of molecular dimensions. Finally, there is no analytical solution available for the time-dependent problem, i.e., kinetic experiments cannot be explained on the basis of this theory so far.

Part of these shortcomings is removed by an alternative theory. Ion movement across the barrier is described by the formalism of chemical kinetics in this case (Ketterer et al., 1971; Läuger and Stark, 1970), i.e.,

$$\Phi = k'_{MS}N'_{MS} - k''_{MS}N''_{MS} \tag{24}$$

with $N'_{MS}$ and $N''_{MS}$ representing interfacial concentrations in the energy minima, and $k'_{MS}$ and $k''_{MS}$ rate constants of ion translocation across the barrier (cf. Figs. 1 and 3). Application of Eq. 24 is only correct if ion concentrations outside the energy minima can be neglected, i.e., in the case of a sufficiently steep and high energy barrier. When this assumption is used, the Nernst-Planck approach and the kinetic approach become equivalent (Ciani et al., 1973; Benz et al., 1976). By comparison of Eqs. 23 and 24, the voltage dependence of the rate constants, $k'_{MS}$ and $k''_{MS}$, is obtained in the form of Eqs. 6 and 7, with

$$k_{MS} = \frac{1}{\vartheta\int_{-\beta d}^{\beta d}(\exp[w(x) - w(\beta d)]/D(x))dx} \tag{25}$$

and

$$f(u) = \frac{\int_{-\beta d}^{\beta d}(\exp[w(x)]/D(x))dx}{\int_{-\beta d}^{\beta d}(\exp[w(x) + z\varphi(x)]/D(x))dx} \tag{26}$$

$\vartheta$ represents a length that is characteristic of the distance between diffusional energy minima.

Equations 25 and 26 may be used to discuss certain limiting cases. For a rectangular barrier of width $b$ and height $w_0$, one obtains (under the assumption of a constant diffusion coefficient, $D$, inside the membrane)

$$k_{MS} = \frac{D}{\vartheta bd}\frac{1}{\exp[w_0 - w(\beta d)]} \tag{27}$$

and

$$f(u) = \frac{zbu/2}{\sinh(zbu/2)} \tag{28}$$

For sufficiently small values of the width $b$, Eq. 28 is reduced to $f(u) = 1$. In this case, Eqs. 6 and 7 correspond to Eyring's treatment of membrane diffusion, which describes ion movement across barriers in terms of single jumps (Zwolinski et al., 1949; Läuger and Stark, 1970). By assuming that $b > 0$, Eq. 28 has been repeatedly applied to explain discrepancies observed between experimental current-voltage curves and a kinetic treatment based on Eyring's theory (Hladky, 1974; Krasne and Eisenman, 1976; Ciani, 1976; Benz and McLaughlin, 1983). In a similar way, the correc-

**TABLE 1 Charge-pulse relaxation data analyzed according to Eq. 21, assuming $\beta = 0.5$**

| Lipid | $\tau_1/\mu s$ | $\tau_2/\mu s$ | $\tau_3/\mu s$ | $\alpha_1$ | $\alpha_2$ |
|---|---|---|---|---|---|
| 18:1 MG ($n$ = 15) | 0.67 ± 0.12 | 5.55 ± 0.35 | 88.6 ± 9.6 | 0.79 ± 0.03 | 0.08 ± 0.014 |
| 20:1 MG ($n$ = 17) | 4.04 ± 0.67 | 10.5 ± 1.77 | 264 ± 9.60 | 0.64 ± 0.08 | 0.10 ± 0.03 |
| 22:1 MG ($n$ = 14) | 3.04 ± 0.48 | 9.60 ± 2.65 | 123 ± 29.3 | 0.84 ± 0.09 | 0.10 ± 0.05 |

Experimental conditions: $5 \times 10^{-4}$ M valinomycin in the membrane-forming solution, 1 M RbCl in water, $T$ = 20°C ($n$ = number of measurements). The initial voltage was less than 20 mV. The data represent mean values with standard deviation.

**TABLE 2 Rate constants obtained from the data in Table 1**

| Lipid | $k_{MS}/10^4$ s$^{-1}$ | $k_S/10^4$ s$^{-1}$ | $k_D/10^4$ s$^{-1}$ | $k_R c_M/10^4$ s$^{-1}$ | $N_o$/pmol cm$^{-2}$ |
|---|---|---|---|---|---|
| 18:1 MG | 14.7 ± 3.4 | 1.55 ± 0.13 | 8.50 ± 1.38 | 9.60 ± 1.01 | 3.35 ± 0.58 |
| 20:1 MG | 3.50 ± 0.31 | 1.16 ± 0.08 | 2.71 ± 0.27 | 6.98 ± 0.40 | 1.29 ± 0.12 |
| 22:1 MG | 1.40 ± 0.25 | 0.94 ± 0.16 | 5.46 ± 2.15 | 5.92 ± 1.63 | 6.16 ± 0.83 |

tion function

$$f(u) = \exp(-\omega u^2) \tag{29}$$

has been used to account for the shape of an image force barrier (Haydon and Hladky, 1972; Andersen and Fuchs, 1975; Hladky, 1974).

In the present study the function $f(u)$ was chosen in the form of Eq. 8. This function has two free parameters and has been found to be flexible enough to account for different shapes of the internal barrier (see below).

The applied formalism allows analysis of both the shape of current-voltage curves and fast kinetic experiments, which were designed to determine the value of the model parameters. The continuum approach, which is based on the Nernst-Planck equation, has been found to provide a better description of current-voltage curves than the pure Eyring formalism (Hall et al., 1973; van Dijk and de Levie, 1985). It has a number of shortcomings, however, which have been summarized above. The modified kinetic approach used in the present study, via Eqs. 25 and 26, connects both treatments and allows a quantitative description of all relevant experiments.

The correction function $f(u)$ obtained by the present analysis (cf. Fig. 7) is clearly different from $f(u) = 1$, which holds for the simple Arrhenius (or Eyring) barrier (assumed throughout earlier interpretations of carrier-mediated transport (Läuger and Stark, 1970; Stark and Benz, 1971). In principle, if $f(u)$ is known, the shape of the potential energy $w(x)$ may be determined by deconvolution of Eq. 26 (assuming $D(x) = D$ as a constant). In practice, however, in view of the limited, experimentally accessible voltage range, there is no unique solution to the problem. This is illustrated as follows. The shape of the experimentally determined function $f(u)$ (i.e., of Eq. 8 with the parameters of Table 4) was found to be hardly distinguishable from Eqs 28 and 29 (cf. Fig. 8). This means that the two kinds of barriers, the rectangular barrier and the image force barrier—within the experimental error—can hardly be distinguished from one another and represent appropriate approximations of the true barrier shape experienced by the carrier complexes. The close correspondence between the true barrier and a rectangular barrier is supported by comparison of the width, $b$, of the rectangular barrier with the constant, $\beta$, which determines the voltage dependence of ion translocation (cf. Fig. 1 and Eqs. 6 and 7). The relative distance, $2\beta = 0.76$ (cf. Table 3), between the two energy minima is only slightly larger than the relative width, $b = 0.66$, of the rectangular barrier (cf. Fig. 8 *a*). The same holds for membranes formed from 20:1 MG ($2\beta = 0.76$, $b = 0.59$, data not shown). A comparatively steep trapezoidal barrier for macrocyclic ion carriers was already deduced throughout an early analysis of the shape of steady-state current-voltage curves, assuming $\beta = 0.5$ (Hall et al., 1973). The present kinetic analysis may be regarded as a generalization of these early efforts, which allows independent determination of the value of $\beta$.

$f(u)$ may also be approximated by Eq. 29, i.e., by assuming the shape of an image force barrier (cf. Fig. 8 *b*). The value obtained for the parameter $\omega$ is larger by a factor of 2–3 as compared with the theory (Haydon and Hladky, 1972; Andersen and Fuchs, 1975). The latter was performed under the assumption $\beta = 0.5$, however, i.e., by neglecting the voltage dependence of the interfacial reaction.

The shapes of the different membrane barriers are illustrated in Fig. 9. Discrimination between them requires initial voltages larger than 300 mV, the maximum voltage applied throughout the charge-pulse experiments of the present study. The shape of the interfacial barriers is tentative. The voltage dependence of the partition coefficient, $\gamma_M$ (Eqs. 9–11), is only a function of the parameter, $\beta$, i.e., it does not depend on the interfacial barrier.

Our study is based on experiments with monoglyceride membranes. This system is most appropriate for the analysis presented, because it shows comparatively large amplitudes of the specific relaxation processes of valinomycin-induced ion transport. The effectiveness of carrier-mediated transport is strongly dependent on the nature of the lipid (Szabo et al., 1973). As a consequence, the rate constants of the model (and therefore the height of the corresponding energy barriers) may change considerably (Benz et al., 1977; Lapointe and Laprade, 1982). Future studies will show whether this also holds for the general shape of the barrier (described by the quantities $g$, $h$, and $\beta$).

**TABLE 3 Rate constants obtained by numerical analysis at the $\beta$ values indicated**

| Lipid | $k_{MS}/10^4$ s$^{-1}$ | $k_S/10^4$ s$^{-1}$ | $k_D/10^4$ s$^{-1}$ | $k_R c_M/10^4$ s$^{-1}$ | $N_o$/pmol cm$^{-2}$ |
|---|---|---|---|---|---|
| 18:1 MG $\beta = 0.35$ ($n = 7$) | 15.7 ± 2.55 | 1.34 ± 0.16 | 4.62 ± 0.79 | 8.84 ± 0.74 | 4.57 ± 0.55 |
| 20:1 MG $\beta = 0.38$ ($n = 8$) | 4.15 ± 1.49 | 0.85 ± 0.19 | 1.52 ± 0.38 | 4.81 ± 0.94 | 1.75 ± 0.72 |
| 22:1 MG $\beta = 0.38$ ($n = 6$) | 2.18 ± 0.38 | 0.64 ± 0.07 | 3.36 ± 0.71 | 2.49 ± 0.43 | 8.38 ± 0.62 |

For experimental conditions, see Table 1.

**TABLE 4 The constants *g* and *h* of Eq. 8**

| | 20:1 MG | 22:1 MG |
|---|---|---|
| *g* | 303.0 ± 0.63 | 588.8 ± 0.88 |
| *h* | 2.7 ± 0.001 | 3.16 ± 0.001 |

The applied carrier model is based on a series of assumptions and simplifications:

1. The time dependence of ion equilibration between the aqueous phase and the interfacial energy minima is neglected. This means that the height of the interfacial barrier is assumed to be smaller than the height of the inner membrane barrier.

2. The dielectric constant, $\epsilon$, was assumed to be voltage independent.

3. A possible voltage dependence of the rate constants $k_R$ and $k_D$ (Hladky, 1974) is neglected. The same holds for the translocation rate constant, $k_S$, of the neutral carrier molecules S. Although these molecules cannot be influenced in a direct way, it cannot be excluded a priori that the movement of neutral molecules is indirectly affected by the application of high membrane voltages, namely via the pressure of the charged membrane capacity. As a consequence of this pressure, voltage-dependent capacitance (or thickness) changes have been reported that depend on the second power of the membrane voltage (see Benz and Janko, 1976; van Dijk and de Levie, 1985; and the discussion in these papers). We think, however, that in the case of very fast charge-pulse experiments, despite the high initial voltage applied, changes in the membrane thickness can be largely neglected. This holds in view of the comparatively long time interval (milliseconds to seconds) required to produce these changes (Benz and Janko, 1976). The membrane voltage in a charge-pulse experiment, however, decays in a time range of less than 1 ms.

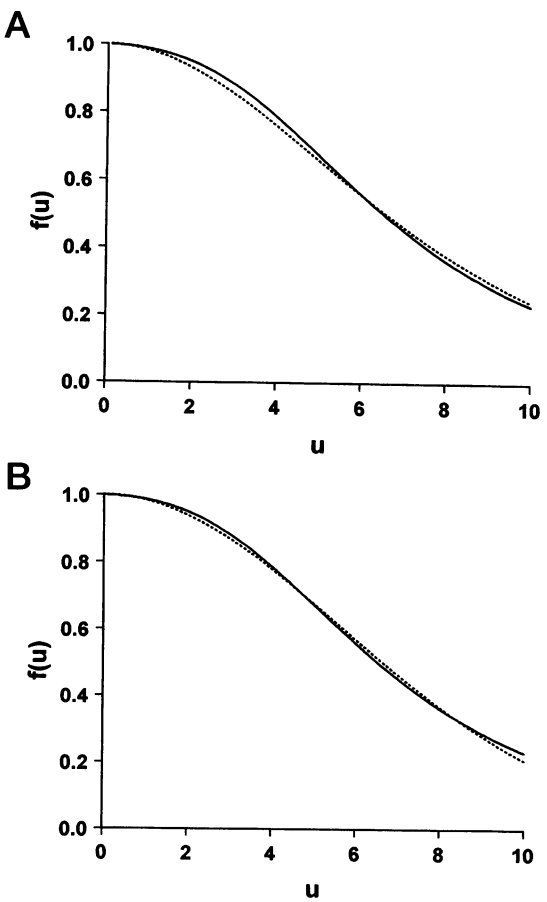


FIGURE 8 Fit of the experimentally determined correction function $f(u)$ for 22:1 MG membranes (——) with Eq. 28 (*a*) ($b$ = 0.66; – – –) and with Eq. 29 (*b*) ($\omega$ = 0.0156; – – –).

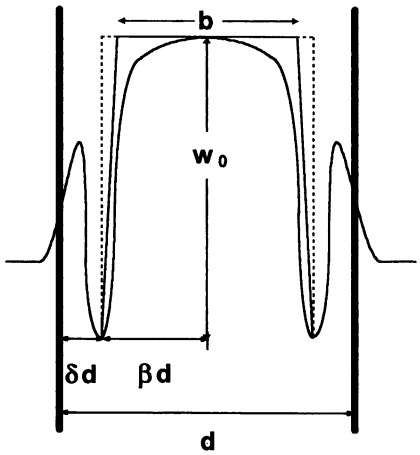


FIGURE 9 Schematic representation of a rectangular barrier, a trapezoidal barrier of height $w_0$ and width $b$, and a tentative image force barrier.

4. Further simplification applies to interfacial complex formation, which is described as a simple bimolecular reaction (cf. Fig. 3). Complex formation has been found, however, to proceed via one or several intermediate states (Grell and Funck, 1973; Grell et al., 1975). The intermediate states may be neglected under certain experimental conditions, if their concentration is comparatively small. In such a case the extended reaction scheme has been found to become kinetically equivalent to the basic four-state model applied in the present study (Knoll and Stark, 1975; Hladky et al., 1995). As a result, the time dependence of the membrane voltage in a charge-pulse experiment is not affected by intermediate states of low concentration. Intermediate states must be considered, however, if the dependence of the relaxation parameters on the ion concentration in water is studied.

Despite the simplifications, the applied model has been found to agree with the experimental data presented. A further refinement of the model would inevitably require introduction of further adaptable parameters which, in view of the limited experimental information available, would give rise to redundancy in determination.

The present analysis is largely based on charge-pulse experiments at high membrane voltages. Similar information is, in principle, available from voltage-jump experiments. The time resolution of this technique, which was

originally used to investigate the kinetics of carrier-mediated ion transport (Stark et al., 1971), is, however, smaller by one order of magnitude at least. The application of high membrane voltages, which is an inevitable requirement for the analysis of the barrier shape (see above), shifts the kinetics of the investigated phenomena into a time range where the improved time resolution of the charge-pulse technique provides a significant advantage.

The authors thank Dr. Nieto Frausto (Puebla, Mexico) for many helpful discussions on the theoretical aspects of the study and Dr. Ingo Wuddel (University of Konstanz) for leaving us a special FORTRAN routine of the Runge-Kutta procedure.

The authors gratefully acknowledge financial support obtained through the Deutsche Forschungsgemeinschaft (under grant Sta 236/3-2).

## REFERENCES

Andersen, O. F., and M. Fuchs. 1975. Potential energy barriers to ion transport within lipid bilayers. Studies with tetraphenylborate. *Biophys. J.* 15:795–830.

Barth, C., H. Bihler, M. Wilhelm, and G. Stark. 1995. Application of a fast charge-pulse technique to study the effect of the dipolar substance 2,4-dichlorophenoxyacetic acid on the kinetics of valinomycin mediated $K^+$-transport across monoolein membranes. *Biophys. Chem.* 54: 127–136.

Benz, R., O. Fröhlich, and P. Läuger. 1977. Influence of membrane structure on the kinetics of carrier-mediated ion transport through lipid bilayers. *Biochim. Biophys. Acta.* 464:465–481.

Benz, R., and K. Janko. 1976. Voltage-induced capacitance relaxation of lipid bilayer membranes. Effect of membrane composition. *Biochim. Biophys. Acta.* 455:721–738.

Benz, R., H.-A. Kolb, P. Läuger, and G. Stark. 1989. Ion carriers in planar lipid membranes: relaxation studies and noise analysis. *Methods Enzymol.* 171:274–286.

Benz, R., and P. Läuger. 1976. Kinetic analysis of carrier-mediated ion transport by the charge pulse technique. *J. Membr. Biol.* 27:171–191.

Benz, R., P. Läuger, and K. Janko. 1976. Transport kinetics of hydrophobic ions in lipid bilayer membranes: charge pulse relaxation studies. *Biochim. Biophys. Acta.* 455:701–720.

Benz, R., and S. McLaughlin. 1983. The molecular mechanism of action of the proton ionophore FCCP (carbonylcyanide *p*-trifluoromethoxyphenylhydrazone). *Biophys. J.* 41:381–398.

Bihler, H. 1996. Ladungspulsexperimente an planaren Lipidmembranen zur Analyse der inneren Membranbarriere für makrozyklische Ionencarrier. Ph.D. thesis. University of Konstanz, Konstanz, Germany.

Ciani, S. 1976. Influence of molecular variations of ionophore and lipid on the selective ion permeability of membranes. II. A theoretical model. *J. Membr. Biol.* 30:45 -63.

Ciani, S., R. Laprade, G. Eisenman, and G. Szabo. 1973. Theory for carrier-mediated zero current conductance of bilayers extended to allow for nonequilibrium of interfacial reactions, spatially dependent mobilities and barrier shape. *J. Membr. Biol.* 11:255–292.

Feldberg, S. W., and G. Kissel. 1975. Charge-pulse studies of transport phenomena in bilayer membranes. I. Steady state measurements of actin- and valinomycin-mediated transport in glycerol monooleate bilayers. *J. Membr. Biol.* 20:269–300.

Grell, E., and T. Funck. 1973. Dynamic properties and membrane activity of ion specific antibiotics. *J. Supramol. Struct.* 1:307–335.

Grell, E., T. Funck, and F. Eggers. 1975. Structure and dynamic properties of ion-specific antibiotics. *In* Membranes. A Series of Advances, Vol. 3. G. Eisenman, editor. Dekker, New York. 1–26.

Hall, J. E., C. A. Mead, and G. Szabo. 1973. A barrier model for current flow in lipid bilayer membranes. *J. Membr. Biol.* 11:75–97.

Haydon, D. A., and S. B. Hladky. 1972. Ion transport across thin lipid membranes: a critical discussion of mechanisms in selected systems. *Q. Rev. Biophys.* 5:187–282.

Hladky, S. B. 1974. The energy barriers to ion transport by nonactin across thin lipid membranes. *Biochim. Biophys. Acta.* 352:71–85.

Hladky, S. B. 1979. The carrier mechanism. *Curr. Top. Membr. Transp.* 12:53–164.

Hladky, S. B. 1992. Kinetic analysis of lipid soluble ions and carriers. *Q. Rev. Biophys.* 25:459–475.

Hladky, S. B., J. C. H. Leung, and W. J. Fitzgerald. 1995. The mechanism of ion conduction by valinomycin: analysis of charge pulse responses. *Biophys. J.* 69:1758–1772.

Ketterer, B., B. Neumcke, and P. Läuger. 1971. Transport mechanism of hydrophobic ions through lipid bilayer membranes. *J. Membr. Biol.* 5:225–245.

Knoll, W., and G. Stark. 1975. An extended kinetic analysis of valinomycin-induced Rb-transport through monoglyceride membranes. *J. Membr. Biol.* 25:249–270.

Krasne, S., and G. Eisenman. 1976. Influence of molecular variations of ionophore and lipid on the selective ion permeability of membranes. I. Tetranactin and the methylation of nonactin-type carriers. *J. Membr. Biol.* 30:1–44.

Lapointe, J. Y., and R. Laprade. 1982. Kinetics of carrier-mediated ion transport in two new types of solvent-free lipid bilayers. *Biophys. J.* 39:141–150.

Läuger, P., R. Benz, G. Stark, E. Bamberg, P. C. Jordan, A. Fahr, and W. Brock. 1981. Relaxation studies of ion transport systems in lipid membranes. *Q. Rev. Biophys.* 14:513–598.

Läuger, P., and G. Stark. 1970. Kinetics of carrier-mediated ion transport across lipid bilayer membranes. *Biochim. Biophys. Acta.* 211:458–466.

Neumcke, B., and P. Läuger. 1969. Nonlinear electrical effects in lipid bilayer membranes. II. Integration of the generalized Nernst-Planck equations. *Biophys. J.* 9:1160–1170.

Smejtek, P. 1995. Permeability of lipophilic ions across lipid bilayers. *In* Permeability and Stability of Lipid Bilayers. E. A. Disalvo and S. A. Simon, editors. CRC Press, Boca Raton, FL. 197–240.

Stark, G. 1984. Hydrophobic ions, carriers and pore formers as studied by fast kinetic methods. *In* Biomembranes: Dynamics and Biology. F. C. Guerra, R. M. Burton, editors. Plenum, New York. 193–224.

Stark, G., and R. Benz. 1971. The transport of potassium through lipid bilayer membranes by the neutral carriers valinomycin and monactin. Experimental studies of a previously proposed model. *J. Membr. Biol.* 5:133–154.

Stark, G., B. Ketterer, R. Benz, and P. Läuger. 1971. The rate constants of valinomycin-mediated ion transport through thin lipid membranes. *Biophys. J.* 11:981–994.

Szabo, G., G. Eisenman, R. Laprade, S. M. Ciani, and S. Krasne. 1973. Experimentally observed effects of carriers on the electrical properties of bilayer membranes—equilibrium domain. *In* Membranes. A Series of Advances, Vol. 2. G. Eisenman, editor. Dekker, New York. 179–328.

van Dijk, C., and R. de Levie. 1985. An experimental comparison between the continuum and single jump descriptions of nonactin-mediated potassium transport through black lipid membranes. *Biophys. J.* 48: 125–136.

Zwolinski, B. J., H. Eyring, and C. E. Reese. 1949. Diffusion and membrane permeability. *J. Phys. Colloid Chem.* 53:1426–1453.